

A Policy-Aware Cross-Layer Auditing Service for Tiering and Throttling in Starlink

Houtianfu Wang, *Student Member, IEEE*, Hanlin Cai, *Student Member, IEEE*, Haofan Dong, *Member, IEEE*, and Ozgur B. Akan, *Fellow, IEEE*

Abstract—We present a policy-aware, cross-layer methodology for edge-side auditing of service tiering and quota-based throttling in Starlink. Using a multi-week plan-hopping campaign (232.8 h) on a UK residential terminal, we align 1 Hz terminal telemetry with host-side probes to obtain portal-labeled traces spanning priority (pre-quota), post-quota throttling, stay-active operation, and residential service. Using portal status only as ground truth (independent of throughput), we show these policy regimes manifest as distinct signatures in goodput, PoP RTT, and an internal-to-user ratio $R = C_{\text{int}}/T_{\text{user}}$. A lightweight rule on windowed medians separates high-speed from low-rate operation without operator visibility.

Index Terms—Starlink, Satellite Communication, Low-Earth orbit, Network Measurement, Network Performance

I. INTRODUCTION

Low-Earth orbit (LEO) constellations are an increasingly important platform for broadband connectivity. Starlink, the largest deployed system to date, presents a familiar retail product to end users (a small terminal and a monthly subscription) but internally exposes multiple tariff tiers, data quotas, and post-quota throttling modes. Beyond headline downlink rates, operators can map these plans to queueing priorities, rate shaping, and fairness policies at the point of presence (PoP). This raises a practical question for edge observers: when user-perceived throughput collapses, can we diagnose whether the link is under policy enforcement (e.g., tiering or throttling), rather than experiencing incidental low-performance episodes (e.g., short congestion, obstruction, or path variation), especially when plan/quota metadata is unavailable or not collected in measurement pipelines? Our focus is policy observability under a controlled plan-hopping design: we test whether portal-defined regimes admit compact edge-side fingerprints, rather than attributing every low-throughput episode in the wild to policy enforcement.

A growing body of measurement work has begun to characterize Starlink’s performance for fixed and mobile users, from early “first look” studies to larger-scale datasets [1], [2], [3]. Most campaigns adopt an end-to-end, black-box view: they establish baselines for latency, throughput, and loss, and document the effects of handovers and routing on user experience. More recent efforts use crowdsourced and geographically

distributed probes to build a global performance picture and compare Starlink against terrestrial access, and “hitchhiking” approaches expand coverage without dedicated terminals [4], [5].

Other studies correlate performance with physical and environmental factors. WetLinks combines long-term measurements with weather records to quantify rain and cloud impact [6], and Ullah et al. evaluate resilience under controlled rain and mobility scenarios [7]. Ramanathan and Abdu Jyothi analyze Starlink during a major solar storm using RIPE Atlas [8], and the Starlink Robot platform enables repeatable vehicular measurements with controlled obstructions [9]. Collectively, these papers show that weather, space weather, and mobility substantially affect performance, but they typically treat commercial plans and quota configuration as fixed background and do not provide a systematic edge-side diagnosis of policy enforcement.

A complementary line of gray-box work leverages terminal-side telemetry and protocol traces to understand the engineering implementation of LEO systems. Reverse engineering of Starlink user terminals highlighted gRPC as a key interface and enabled subsequent telemetry-driven measurement tools [10]. LENS combines terminal internal metrics with outside-in active probes at scale [11], while other efforts study routing behavior and fine-grained downlink patterns using network- and PHY/transport-level traces [12], [13]. Building on these measurements, SatPipe proposes LEO-aware transport designs [14], and trace-driven emulation frameworks improve reproducibility for satellite networks [15]. This line of work focuses on topology, scheduling, congestion control, and emulation, rather than on how commercial service tiers and quota policies are implemented and exposed on the wire as edge-diagnosable signals.

To address this gap, we introduce a policy-aware, cross-layer measurement methodology that drives a single terminal through different tariff and quota states while aligning terminal-side telemetry with host-side probes. On a residential Starlink deployment in the UK, a multi-week plan-hopping campaign exercises stay-active, priority, post-quota throttling, and residential service. The resulting traces reveal stable, state-dependent fingerprints in download throughput, RTT to the PoP, and an internal-to-user ratio $R = C_{\text{int}}/T_{\text{user}}$ that combines terminal telemetry with host-side goodput. Here T_{user} is the host-side TCP goodput from active throughput tests, while C_{int} is an internal downlink throughput indicator taken from the telemetry field `downlink_throughput_bps` (converted to Mbps); accordingly, R should not be interpreted as protocol

H. Wang, H. Cai, H. Dong, and O. B. Akan are with the Internet of Everything Group, Department of Engineering, University of Cambridge, Cambridge CB3 0FA, U.K. (e-mail: {hw680, hc663, hd489}@cam.ac.uk; oba21@cam.ac.uk).

O. B. Akan is also with the Center for neXt-generation Communications (CXC), Department of Electrical and Electronics Engineering, Koç University, Istanbul 34450, Turkey.

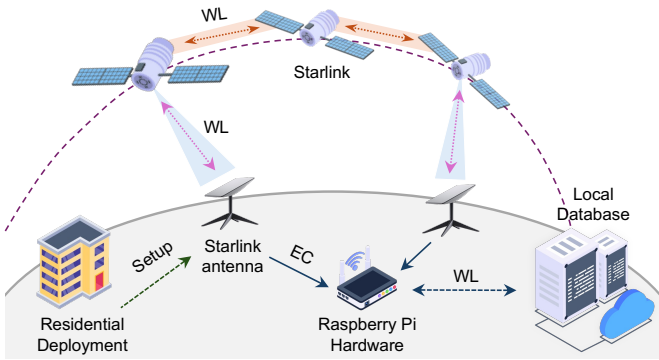


Fig. 1: Starlink deployment and measurement setup (WL: Wireless Link, EC: Ethernet Connection).

header overhead. We use portal status only for ground-truth labeling in this study; the detector itself relies on short windowed throughput tests and local telemetry. We report a single-site case study: the alignment procedure is reusable, but numerical thresholds and values are deployment-specific.

On this deployment and dataset, we make three observations. First, portal-labeled plan/quota regimes manifest as three dominant operating signatures on this trace: two low-rate regimes (stay-active and post-quota throttled) and a high-speed regime (priority/residential), with distinct PoP RTT and R characteristics. On this deployment, the two low-rate regimes typically appear as stable plateaus (around 0.5 Mbps for stay-active and around 1 Mbps for post-quota throttling), but these values are empirical signatures rather than labeling criteria. Second, quota depletion is followed by a short enforcement-delay window and then a sharp drop in user goodput accompanied by a step change in R , aligned with the portal-reported transition into post-quota throttling on this trace. Third, the joint space of download goodput and R forms well-separated clusters for these portal-defined regimes, enabling a simple threshold-based heuristic to distinguish low-rate from high-speed windows and, on this dataset, to differentiate the two low-rate regimes. Together, these results provide a compact starting point for replicable edge-side auditing of tariff and quota policies on LEO access links and motivate exploring such fingerprints in future constellations.

II. METHODOLOGY

A. Deployment and measurement host

As shown in Fig. 1, we deploy our measurement infrastructure in a representative real-world Starlink residential environment located at University of Cambridge with open-sky view and no persistent line-of-sight obstructions. A Raspberry Pi 5 connects to the terminal via wired Ethernet and serves as a dedicated measurement host. The subscription is not shared with other clients during experiments, and all logs are timestamped in UTC (NTP-synchronized).

B. Terminal telemetry

We collect terminal-side telemetry using `starlink-gRPC-tools` [16] with a 5 s polling interval, stored in a local SQLite

database. We additionally enable bulk-history export to obtain 1 Hz time series including internal downlink/uplink throughput indicators, PoP-side RTT/loss statistics, and scheduling/obstruction flags.

C. Host-side active probing

On the same Raspberry Pi, a Python client performs end-to-end probing. Every $\sim 4\text{--}5$ s it issues a short ICMP ping train (4 probes) to a public DNS resolver and records average RTT and loss. Every 120 s it runs `speedtest-cli` (default server selection) to obtain downstream and upstream TCP goodput. The client also reads Ethernet interface byte counters to estimate access-link send/receive throughput. All records use UTC timestamps to align host-side observations with terminal telemetry.

D. Policy-aware labeling via plan hopping

We run telemetry and probing continuously for multiple weeks (232.8 hours total). To exercise tariff- and quota-driven behavior, we perform plan-hopping experiments that drive the same subscription through stay-active, priority (pre-quota), a short post-depletion enforcement delay window G , post-quota throttling, and residential service. Each plan-to-plan switch is repeated 5 times. We use Starlink account-portal status only for ground-truth labeling and align portal events with the telemetry/probing logs.

We define a stable segment as a contiguous interval where the portal-reported plan/quota state is unchanged. To avoid conflating transient effects near portal transitions with steady-state regimes, we discard a guard interval of ± 120 s around each portal state change and label only the remaining intervals of length $\geq T_{\min}$; in our dataset, the minimum stable-segment length is approximately 1 h 18 m 50 s. The low-rate plateaus reported in Sec. III are empirical signatures of these portal-defined regimes on this deployment, not a labeling criterion.

For each stable segment, we assign one of the following nominal states based on the portal-reported plan/quota status:

- S1 (stay-active): portal-reported stay-active regime.
- S2 (priority): pre-quota priority regime.
- S3 (post-quota throttled): portal-reported post-quota throttling regime.
- S4 (residential): portal-reported residential regime.

In subsequent analysis, S2 and S4 form a combined high-speed regime (S2/S4), while S1 and S3 are the two low-rate regimes. On this trace, S1 and S3 typically appear as stable low-rate plateaus around 0.5 Mbps and 1 Mbps, respectively.

III. SERVICE DIFFERENTIATION ACROSS TARIFF STATES

This section characterizes observable differences of the same terminal under different tariff and quota configurations, focusing on end-to-end performance, terminal-side telemetry, and the dynamics around quota depletion.

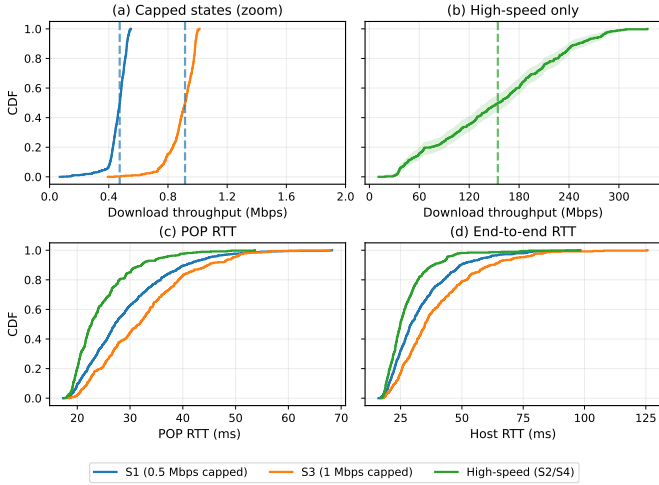


Fig. 2: Download throughput and RTT distributions across representative tariff states.

A. End-to-end performance across states

Fig. 2 characterizes three separable operating regimes for this terminal using download throughput and RTT distributions. Fig. 2(a) focuses on the two low-rate regimes (S1 and S3): their throughput samples concentrate tightly, forming two narrow plateaus in the low-throughput region (centered around ~ 0.5 Mbps and ~ 1 Mbps, respectively). Fig. 2(b) shows that the high-speed regime (S2/S4) occupies a much wider region, with most samples between a few tens and a few hundred Mbps, clearly separated from the low-rate plateaus. Table I summarizes the per-state distributions. S2/S4 sustains substantially higher downlink rates and the lowest median RTT at both host and PoP.

The RTT CDFs in Fig. 2(c) and Fig. 2(d) follow the same separation pattern: the curves for S2/S4 are shifted left, while S1 and especially S3 extend further into the tail. Overall, for this terminal and dataset, the portal-defined regimes manifest as three dominant signatures in the throughput–latency space: two narrow low-rate plateaus and a wide high-speed cluster at the hundred-Mbps scale.

B. Terminal telemetry and the internal-to-user ratio

Throughput and RTT alone are often insufficient for a runtime diagnosis of whether a low-throughput interval reflects policy enforcement or an incidental episode (e.g., short congestion, obstruction, or shared-load effects). We therefore incorporate terminal-side telemetry and compare a terminal-reported internal downlink indicator against the user-visible goodput.

Fig. 3 shows the distribution of an internal-to-user ratio

$$R = \frac{C_{\text{int}}}{T_{\text{user}}},$$

where T_{user} is the host-side TCP goodput from our active throughput tests and C_{int} is a terminal-reported internal downlink throughput indicator (e.g., `download_throughput_bps`). C_{int} is a terminal-reported

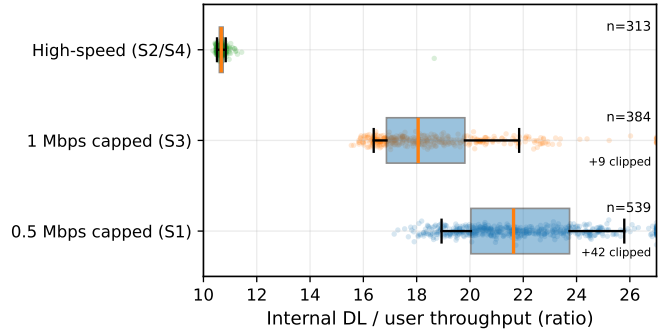


Fig. 3: Distribution of the internal-to-user ratio $R = C_{\text{int}}/T_{\text{user}}$ across tariff states, where C_{int} is a terminal-reported internal downlink indicator and T_{user} is host-side TCP goodput. Ratios are clipped for visualization; clipped counts are annotated.

internal downlink indicator, whereas T_{user} is end-to-end payload goodput.

In the high-speed state S2/S4, R is tightly concentrated around 10.7, with 10th–90th percentiles between 10.5 and 10.8. In contrast, the low-rate regimes exhibit substantially larger ratios, with a median around 21.6 for S1 and 18.1 for S3. Together with PoP RTT statistics in Table I, this yields two observations. First, high-speed operation exhibits a remarkably stable ratio around 10.7 on this dataset. One possible explanation is that C_{int} is a terminal-internal indicator whose absolute scale is not directly comparable to end-to-end payload goodput; we do not attempt to interpret its physical semantics. We therefore use $R \approx 10.7$ only as an empirical baseline on this trace, not as a statement about protocol overhead. Second, the upward shift of R in low-rate regimes forms an almost disjoint gap from high-speed operation, making R a compact cross-layer feature for the detector in Section IV.

C. Quota depletion and enforcement-delay behavior

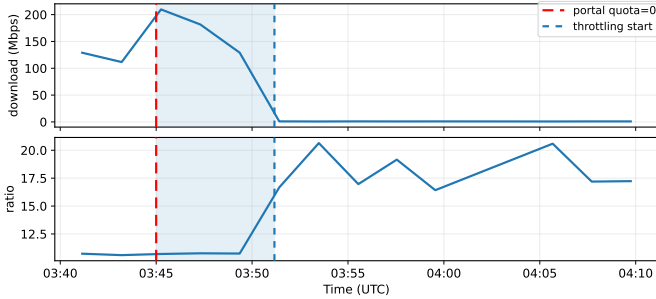
To examine the dynamics after priority quota depletion, Fig. 4 zooms into one quota-depletion instance on November 8, 03:40–04:10 UTC, aligning download throughput, the ratio R , and the portal’s quota indicator. The red vertical line marks the time when the portal reports zero remaining quota, the blue vertical line marks the onset of the 1 Mbps cap, and the shaded region highlights the interval between the two (window G).

In this instance, immediately following the quota depletion report (red line), the download throughput does not instantly collapse. Instead, it remains in the high-speed regime for several minutes, gradually declining from ~ 200 Mbps to ~ 120 Mbps, before abruptly dropping to the 1 Mbps plateau at the throttling onset (blue line). This behavior is consistent with an enforcement delay between quota accounting updates and scheduler-side policy activation on this trace.

The ratio R provides a synchronous signal for the transition. During both the pre-quota and enforcement-delay phases, R stays at the low values characteristic of high-speed operation. Once throttling starts, R quickly jumps to the higher plateau

TABLE I: Per-state summary of throughput, RTT, PoP RTT, and internal-to-user ratio.

State	Download Mbps (median [p10, p90])	Host RTT ms (median [p10, p90])	PoP RTT ms (median [p10, p90])	R (median [p10, p90])
S1	0.4737 [0.4093, 0.5226]	29.168 [20.3088, 49.4734]	27.1594 [20.1335, 40.4985]	21.6361 [18.9336, 25.7945]
S2 and S4	154.4406 [46.1167, 250.0403]	24.911 [19.0640, 38.3970]	22.6937 [19.2297, 32.0950]	10.6677 [10.5086, 10.8386]
S3	0.9153 [0.7746, 0.9853]	34.861 [22.6218, 61.7638]	31.6251 [21.8994, 44.7726]	18.0572 [16.3819, 22.0066]

Fig. 4: Quota depletion, enforcement-delay window G , and throttling onset for the priority plan.

associated with the 1 Mbps low-rate regime. Along the time axis, the joint evolution of throughput and R reveals a three-stage process: quota reaches zero, followed by a high-speed enforcement-delay window G , and finally a strict cap. We report this as a case-study observation on this dataset: it indicates a minutes-scale gap between portal quota status and throttling onset that can be captured by lightweight active measurements.

IV. A LIGHTWEIGHT POLICY-STATE DETECTOR

Section III revealed structured differences in throughput, RTT, and the internal-to-user ratio R across states. This section operationalizes these differences into an edge-side detector: service states form separable fingerprints in a low-dimensional feature space and can be identified with a simple rule.

We focus on three representative regimes: the low-rate stay-active state (S1), the low-rate post-quota throttled state (S3), and the high-speed regime (S2/S4) that covers priority before quota depletion, the enforcement-delay window G , and residential high-speed operation. In the detector, we treat G as part of high-speed operation.

A. A parsimonious black-box interpretation

Fig. 2, Fig. 3, and Table I together suggest a consistent empirical picture. In high-speed operation (S2/S4 and G), download throughput spans tens to hundreds of Mbps, R concentrates tightly around a stable baseline near 10.7, and PoP RTT is lowest. In low-rate operation (S1 and S3), throughput collapses to narrow plateaus, R shifts upward to much larger values, and PoP RTT increases.

These joint signatures are consistent with policy enforcement that limits user-visible goodput without proportionally reducing a terminal-reported internal downlink indicator, yielding an elevated R , and that may also stratify queuing behavior across tiers. A token-bucket and priority-queuing abstraction provides one parsimonious interpretation of the observed plateaus and RTT stratification; however, we do not

attempt to recover or validate the operator’s internal scheduler. Our goal is to extract stable, edge-observable fingerprints that enable runtime diagnosis.

B. Service-tier fingerprints and a decision rule

We now demonstrate that the regimes can be distinguished using only short active tests and local telemetry, without knowledge of the operator’s internal scheduler. To emulate a “user runs a speedtest” scenario, we partition the measurement trace into fixed-length windows of $W = 180$ s with a step of 180 s (non-overlapping).

For each window, we extract two features:

- the median download throughput (Mbps) from the active throughput tests;
- the median ratio R (dimensionless) computed at active-test timestamps by aligning the nearest telemetry sample within ± 10 s.

We visualize these windows in the two-dimensional feature space shown in Fig. 5. Windows from the high-speed regime (S2/S4) cluster in a region of high throughput and low R , while windows from the low-rate regimes (S1/S3) cluster in a region of low throughput and high R .

The separation is sufficiently wide that complex machine learning is unnecessary. Using the empirical distributions in Table I, we define conservative static thresholds: a download threshold $T_d = 50$ Mbps and a ratio threshold $T_r = 14.5$. Table I reports per-sample statistics, whereas our detector operates on windowed medians, which are less sensitive to short bursts when multiple samples fall within a window. The chosen thresholds are therefore conservative for the windowed features. The thresholds are chosen to lie inside the observed gap on this dataset (e.g., the 10th percentile throughput in S2/S4 is ≈ 46 Mbps, while the 90th percentile of R in S2/S4 is ≈ 10.84), providing guardrails against short transient fluctuations.

We label a window as high-speed only if throughput $> T_d$ and $R < T_r$. On the labeled windows in our dataset, we observe no errors for separating the high-speed regime (S2/S4) from the low-rate regimes (S1/S3) on this trace; we use it as a deployment-specific heuristic rather than a universal classifier. The low-rate states S1 and S3 are further distinguished by their low-rate plateaus (around 0.5 Mbps versus around 1 Mbps) on this deployment, reflecting two different portal-defined capped regimes. Overall, for this terminal and deployment, the service state is exposed as a linearly separable fingerprint in the (throughput, R) space; we emphasize that numerical thresholds are deployment-specific and should be re-calibrated when transferred to other environments.

V. DISCUSSION AND CONCLUSION

Previous sections introduced an edge-side, fingerprint-based policy-state detector. We now discuss design implications, limits of interpretation, and extensions of this baseline.

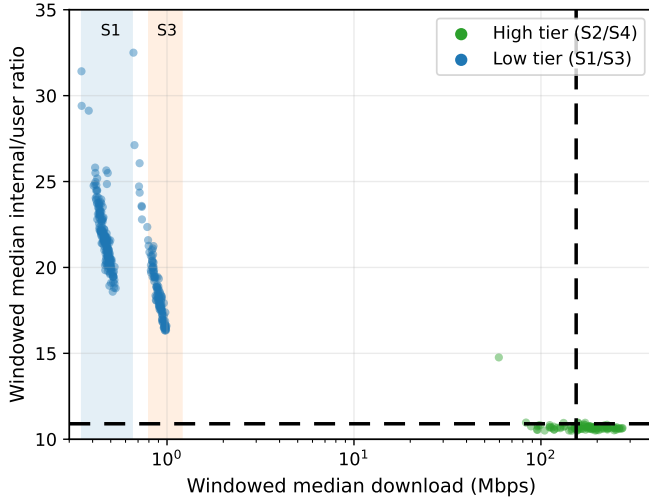


Fig. 5: Service-tier fingerprints in the (throughput, R) feature space. High-speed and low-rate regimes form disjoint clusters on our dataset; the horizontal and vertical thresholds (T_d, T_r) illustrate a conservative decision rule.

A. Design implications

On our dataset, service states form near-disjoint clusters in the two-dimensional space spanned by download goodput and the internal-to-user ratio R . This low-dimensional structure suggests a practical diagnostic primitive: when comparable terminal telemetry is available, short windowed tests combined with simple thresholds can separate high-speed from low-rate operation on a given link, without visibility into the operator’s internal scheduler. The same low-rate plateaus can further distinguish S1 from S3 on this deployment.

B. Limitations and transferability

This study is a single-site, single-terminal case study over a multi-week trace and a finite set of tariff/quota configurations. Accordingly, the numerical values and thresholds reported here should not be read as a global characterization of Starlink policies. Our contribution is methodological: a policy-aware auditing template that aligns portal state, terminal telemetry, and host-side probes via plan hopping, and distills low-dimensional fingerprints using R . In particular, we aim to audit portal-defined tariff and quota regimes under controlled plan changes, rather than to provide a universal classifier that attributes all low-throughput episodes in the wild to policy enforcement.

Thresholds are expected to depend on load, firmware, hardware, and the local network path, and therefore must be recalibrated when transferred to other deployments. Applying the same methodology across additional locations, terminals, and other LEO systems is left for future work.

C. Conclusion

Using one residential Starlink terminal and a policy-aware plan-hopping campaign, we examined how tariff and quota configurations manifest in edge-observable metrics on a live

LEO access link. By aligning terminal telemetry with host-side probes, we identified three stable operating regimes and showed that a two-dimensional feature space spanned by download goodput and R yields an approximately linearly separable fingerprint on this dataset. Compared to prior Starlink measurements focused on coverage, topology, or environmental factors, our results add a policy-observability dimension and distill a minimal edge-side recipe: drive the terminal through available states, collect cross-layer telemetry, and recover low-dimensional signatures for each regime. While the thresholds are deployment-specific, the procedure provides a compact starting point for replicable edge-side auditing across LEO access links.

REFERENCES

- [1] F. Michel, M. Trevisan, D. Giordano, and O. Bonaventure, “A first look at starlink performance,” in *Proceedings of the 22nd ACM Internet Measurement Conference*, 2022, pp. 130–136.
- [2] N. Mohan, A. E. Ferguson, H. Cech, R. Bose, P. R. Renatin, M. K. Marina, and J. Ott, “A multifaceted look at starlink performance,” in *Proceedings of the ACM Web Conference 2024*, 2024, pp. 2723–2734.
- [3] A. E. Ferguson, N. Mohan, H. Cech, R. Bose, P. R. Renatin, M. K. Marina, and J. Ott, “Starlink performance from different perspectives,” in *Proceedings of the 30th Annual International Conference on Mobile Computing and Networking*, 2024, pp. 1662–1664.
- [4] L. Izhikevich, M. Tran, K. Izhikevich, G. Akiwate, and Z. Durumeric, “Democratizing LEO satellite network measurement,” *Proceedings of the ACM on Measurement and Analysis of Computing Systems*, vol. 8, no. 1, pp. 1–27, 2024.
- [5] Y. Wu, M. Cui, G. Gou, Y. Wei, G. Xiong, Z. Li, X. Ju, and W. Xia, “Beneath the heavens: A thorough measurement study of the starlink terrestrial network,” in *Proceedings of the 33rd IEEE/ACM International Symposium on Quality of Service (IWQoS)*. IEEE, 2025, pp. 1–10.
- [6] D. Laniewski, E. Lanfer, B. Meijerink, R. van Rijswijk-Deij, and N. Aschenbruck, “Wetlinks: a large-scale longitudinal starlink dataset with contiguous weather data,” *arXiv preprint arXiv:2402.16448*, 2024.
- [7] M. Asad Ullah, A. Heikkinen, M. Uitto, A. Anttonen, and K. Mikhaylov, “Impact of weather on satellite communication: Evaluating starlink resilience,” *arXiv e-prints*, pp. arXiv–2505, 2025.
- [8] A. Ramanathan and S. Abdu Jyothi, “Weathering a solar superstorm: Starlink performance during the may 2024 storm,” in *Proceedings of the 2nd International Workshop on LEO Networking and Communication (LEO-NET ’24)*. ACM, 2024, pp. 31–36.
- [9] B. Liu, Q. Zhang, Q. Yang, J. Jiao, J. Chauhan, and D. Kanoulas, “The starlink robot: A platform and dataset for mobile satellite communication,” *arXiv preprint arXiv:2506.19781*, 2025.
- [10] M. Rajiullah, G. Caso, A. Brunstrom, J. Karlsson, S. Alfredsson, and O. Alay, “Carl-w: a testbed for empirical analyses of 5g and starlink performance,” in *Proceedings of the 3rd ACM Workshop on 5G and Beyond Network Measurements, Modeling, and Use Cases*, 2023, pp. 1–7.
- [11] J. Zhao and J. Pan, “Lens: A leo satellite network measurement dataset,” in *Proceedings of the 15th ACM Multimedia Systems Conference*, 2024, pp. 278–284.
- [12] B. Wang, X. Zhang, S. Wang, L. Chen, J. Zhao, J. Pan, D. Li, and Y. Jiang, “A large-scale ipv6-based measurement of the starlink network,” *arXiv preprint arXiv:2412.18243*, 2024.
- [13] T. Zimmermann, E. Lanfer, D. Laniewski, S. Brinkmann, and N. Aschenbruck, “Better fill up your pipe-revisiting starlink’s burst characterization,” in *Proceedings of the 2025 3rd Workshop on LEO Networking and Communication*, 2025, pp. 36–42.
- [14] D. Zhao, X. Zhang, and M. Lee, “Satpipe: Deterministic tcp adaptation for highly dynamic leo satellite networks,” in *IEEE INFOCOM 2025-IEEE Conference on Computer Communications*. IEEE, 2025, pp. 1–10.
- [15] W. Tian, Y. Li, J. Zhao, S. Wu, and J. Pan, “An ebpf-based trace-driven emulation method for satellite networks,” *IEEE Networking Letters*, 2024.
- [16] S. a. contributors, “starlink-grpc-tools: Tools for interacting with the starlink user terminal grpc service,” <https://github.com/sparky8512/starlink-grpc-tools>, 2025, accessed: 2025-11-18.